Wei *et al. AMB Expr (2018) 8:72*
https://doi.org/10.1186/s13568-018-0604-5

AMB Express

ORIGINAL ARTICLE

Open Access

Evaluation of anthocyanins in *Aronia melanocarpa*/BSA binding by spectroscopic studies

Jie Wei*, Dexin Xu, Xiao Zhang, Jing Yang and Qiuyu Wang*

Abstract

The interaction between Anthocyanins in *Aronia melanocarpa* (AMA) and bovine serum albumin (BSA) were studied in this paper by multispectral technology, such as fluorescence quenching titration, circular dichroism (CD) spectroscopy and Fourier transform infrared spectroscopy (FTIR). The results of the fluorescence titration revealed that AMA could strongly quench the intrinsic fluorescence of BSA by static quenching. The apparent binding constants K_{SV} and number of binding sites n of AMA with BSA were obtained by fluorescence quenching method. The thermodynamic parameters, enthalpy change (ΔH) and entropy change (ΔS), were calculated to be 18.45 kJ $mol^{-1} > 0$ and 149.72 J mol^{-1} $K^{-1} > 0$, respectively, which indicated that the interaction of AMA with BSA was driven mainly by hydrophobic forces. The binding process was a spontaneous process of Gibbs free energy change. Based on Förster's non-radiative energy transfer theory, the distance r between the donor (BSA) and the receptor (AMA) was calculated to be 3.88 nm. Their conformations were analyzed using infrared spectroscopy and CD. The results of multispectral technology showed that the binding of AMA to BSA induced the conformational change of BSA.

Keywords: Anthocyanins in *Aronia melanocarpa*, BSA, Binding mode, Circular dichroism, Molecular docking

Introduction

Aronia melanocarpa Elliot, a member of the *Rosaceae* family, *Aronia melanocarpa* fruits are one of the richest plant sources of anthocyanins, AMA are water-soluble plant pigments, it has gained popularity due to their high content anthocyanins with antioxidant anti-inflammatory, antimicrobial, hepatoprotective, gastroprotective and other activities (Malinowska et al. 2013; Fares et al. 2011; Kokotkiewicz et al. 2010; Chrubasik et al. 2010). AMA have the better abilities on scavenging free radicals, improving immunity, anti-cancer, anti-aging, anti-cardiovascular disease and so on (Wei et al. 2017, 2016). The basic structure of AMA shown in Scheme 1, the main components of its monomer are cyanidin-3-*O*-arabinoside, cyanidin-3-*O*-galactoside, cyanidin-3-*O*-glucoside and cyanidin-3-*O*-Xyloside. In our previous study, we have carried out a series of optimization on the extraction and purification of AMA, its composition and biological activity were initially identified and studied (de Santiago et al. 2014). Based on this study, it was found that AMA can inhibit the occurrence of diabetes and obesity, and regulate the metabolism balance and the stability of the redox system, we also carried out AMA on mouse aging mechanism of intervention. Research also shows AMA can be used as food additives owing to its strong antioxidant capacity (Hassellund et al. 2012).

Bovine serum albumin (BSA), one of the major components in plasma protein, is the most extensively studied serum albumin, due to its structural homology with HAS(Manikandamathavan et al. 2017). we investigated the binding and associated energy transfer effects of AMA with BSA. A model of this interaction is proposed in which the intrinsic fluorescence of BSA has been quenched by AMA binding by a static quenching procedure. It was found that the hydrophobic interaction between AMA and BSA played a major role in combination of thermodynamic parameters. FTIR and CD analysis showed that AMA significantly affected the polarity

*Correspondence: J.Wei2015@hotmail.com; qiuyuwang@lnu.edu.cn
School of Life Science of Liaoning University, Chongshan Middle road 66, Huanggu District, Shenyang 110036, Liaoning, China

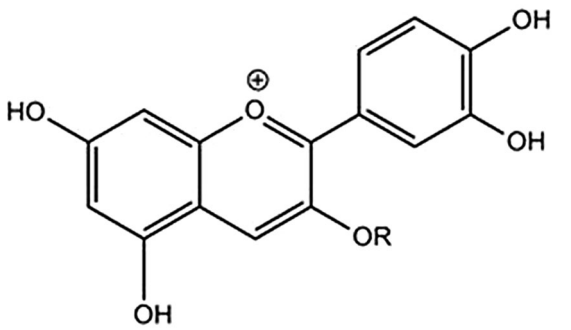

1. R = galactose: Cyanidin 3-galactoside
2. R = glucose: Cyanidin 3-glucoside
3. R = arabinose: Cyanidin 3-arabinoside
4. R = xylose: Cyanidin 3-xyloside

Scheme 1 The structure of anthocyanins

and hydrophobicity of tyrosine and tryptophan in BSA, which could influence the composition of BSA secondary structure, alter the conformation of protein, and further confirm the interaction between AMA and BSA.

The binding of AMA to BSA can alter the pharmacology and pharmacodynamics of these compounds such as their distribution. Therefore, the study of interaction between AMA and BSA binding through spectroscopic techniques is necessary, It laid the foundation for the study of the stability of AMA and BSA (Zhang et al. 2008a, b; Zhang et al. 2012; Sedighipoor et al. 2017).

Materials and methods

Bovine serum albumin (BSA) was purchased from Xi'an Rui Xi Biological Technology Co., Ltd; *Aronia melanocarpa* Elliot fruit was provided by Liaoning Academy of Forestry (Shenyang, China); Anthocyanin standards (cyanidin-3-*O*-arabinoside, cyanidin-3-*O*-galactoside, cyanidin-3-*O*-glucoside and cyanidin-3-*O*-Xyloside) were purchased from Weikeqi Biotechnology Co., Ltd.

Fluorescence quenching titration

5.0 mL anthocyanins solution (1.0 μM) was titrated by successive additions of BSA solution with the concentration of 1.0×10^{-5} mol L^{-1} at different conditions (T = 297, 317, 337 K). The fluorescence quenching of Bovine serum albumin (BSA) with the addition of AR1/AG 50 was recorded in the range of 290–450 nm by fluorescence spectrofluorimeter. The width of the excitation and emission slit was adjusted at 5 nm, and the excitation wavelength was selected at 280 nm. The temperature of samples was kept by recycle water during the whole experiment. All fluorescence titration experiments were done manually by 100 mL microsyringe (Zhang et al. 2013).

Fourier transform infrared spectroscopy (FTIR) analysis

FTIR spectra of AMA and BSA were recorded on Nicolet-6700. FTIR spectrometer via the attenuated total reflection (ATR) at a resolution of 4 cm^{-1} and 32 scans in the range of 400–4000 cm^{-1} at room temperature. The corresponding absorbance contributions of BSA and Anthocyanins solutions were recorded and digitally subtracted with the same instrumental parameters, and their FTIR spectra was done by OMNIC (Li et al. 2016).

Circular dichroism (CD) studies

The optical chamber of the CD spectrometer was deoxygenated with dry nitrogen before used and kept in a nitrogen atmosphere during experiments. The scanning speed was 60 nm min^{-1}, the spectral resolution was 0.2 nm, the response time was 0.25 s, and the slit width was 1 nm. The samples were scanned at 190–250 nm. The composition and content of the secondary structure of the protein were fitted using the Origin program, and the CDpro software was used to fit the protein (BSA) secondary structure.

Molecular docking studies

Molecular docking were carried out to visualize the binding site of AMA to BSA. All the docking calculations were performed by using Autodock 4.2.1.5 Tools (Molecular Graphics Laboratory, The Scripps Research Institute). The 3D structure of four anthocyanins was downloaded from PUBCHEM-OPEN CHEMISTRY DATABASE (https://pubchem.ncbi.nlm.nih.gov/substance). Both BSA and four anthocyanins molecules were prepared using AutoDockTools 1.5.6 before docking, The docking was carried out with $126 \times 126 \times 126$ 0.375 Å spacing grids covering the entire surface of BSA. The Lamarckian genetic algorithm, which is considered one of the most appropriate docking methods available in AutoDock, was used in the docking analysis (Paul et al. 2017).

Molecular dynamic (MD) simulations

The results of Molecular docking simulations determine a general binding mode of ligand. Nevertheless, MD simulation on the ligand–protein complex for further investigation of the effects of ligand binding on the conformation of protein was used. A MD simulation was performed using the AutoDockTools-1.5.6 software package. The crystal structure of BSA complex was downloaded from the Protein Data Bank (RCSB). The model of four anthocyanins monomer were constructed using the Chem3D 16.0 software package (Zhang et al. 2015).

Results

Fluorescence spectra of interaction between different anthocyanins in *Aronia melanocarpa* and BSA

Qualitative analysis of binding of AMA to BSA can be detected by examining fluorescence spectra. Generally, the fluorescence of protein is caused by three intrinsic fluors present in the protein, such as tryptophan, tyrosine, and phenylalanine residues. The fluorescence quenching pattern of BSA was shown in Fig. 1. The figure showed the fluorescence spectrum of the protein when the excitation wavelength is 280 nm, the maximum fluorescence emission wavelength (λ_{max}) of BSA is about 330 nm. The fluorescence intensity at λ_{max} decreases with the increase of anthocyanin concentration, and λ_{max} has red shift phenomenon, which indicates that the microenvironment near the tryptophan and tyrosine residues in this protein was enhanced and the hydrophobicity was decreased. With the increase of the concentration of arabinoside and glucoside, the λ_{max} of BSA appeared blue shift, indicating that the polarity of the binding cavity near the tryptophan residue was weakened and the secondary structure changed (Gallo et al. 2013). In Fig. 1, the λ_{max} of BSA did not change significantly, indicating that the microenvironment of the tryptophan residue did not change. According to the fluorescence data of $\lambda_{ex}=280$ nm, the quenching rates of cyanidin-3-*O*-arabinoside, cyanidin-3-*O*-galactoside, cyanidin-3-*O*-glucoside and cyanidin-3-*O*-Xyloside were 25, 31, 30, 32%. Different quenching rates may be related to the reaction process, the results showed that the quenching rate: The extent of reaction cyanidin-3-i-Xyloside and BSA was the most obvious (Zhang et al. 2008a, b; Unnikrishnan et al. 2014).

Quenching mechanism of BSA fluorescence by AMA

From Fig. 2 it is clear that fluorescence of BSA has been completely quenched by Anthocyanins. The quenching constants has been calculated according to the Stern–Volmer equation Eq. (1),

$$F_0/F = 1 + K_{SV} \cdot C_q = 1 - K_q \tau_0 C_q \quad (1)$$

wherein, F and F_0 are the fluorescence intensity before and after the action of the fluorescence quencher molecule, K_{SV} is the Stern–Volmer dynamic quenching constant, C_q is the quencher concentration, K_q is the rate constant of the biological macromolecule quenching process, τ_0 is the lifetime of the fluorescent molecules (10^{-8} s) when the quencher is absent. According to the formula, the Stern–Volmer (S-V) curve of BSA interacting with four monomer can be obtained by plotting F_0/F

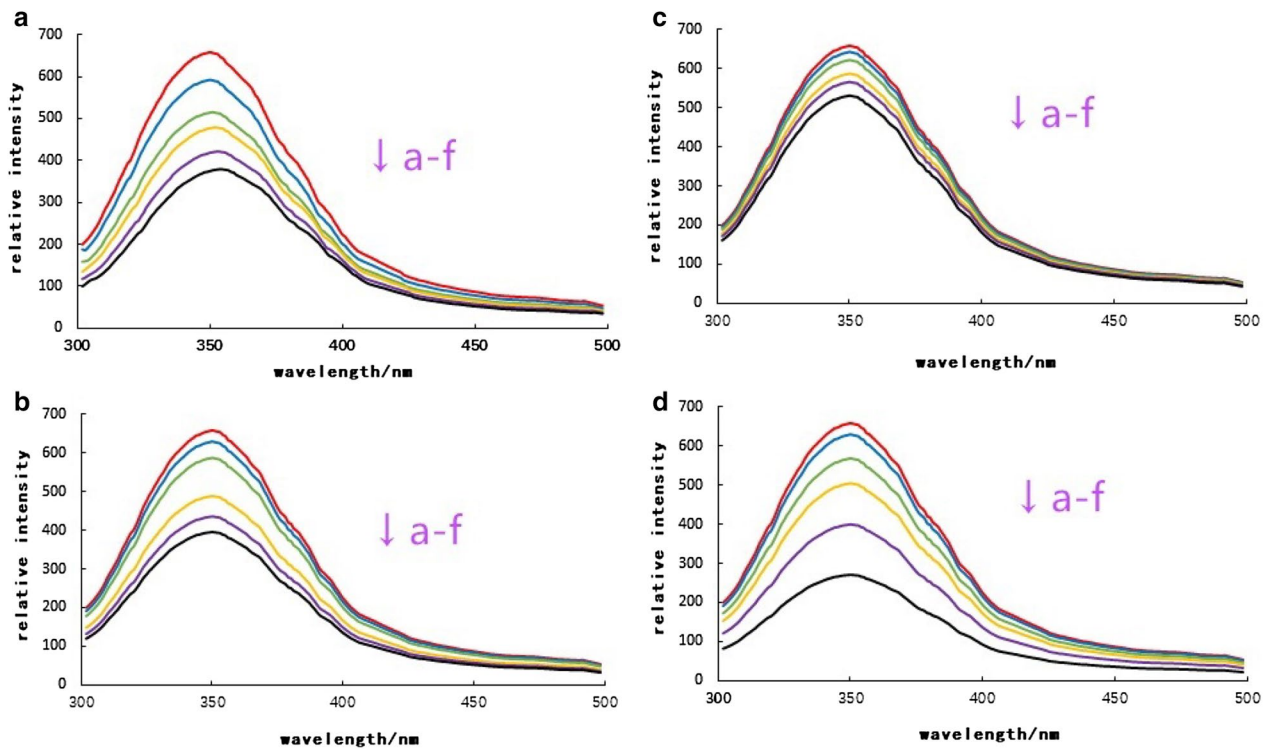

Fig. 1 Fluorescence emission spectra of BSA suspension at excitation wavelength 280 nm in presence of 0, 5, 10, 20, 30, 40 μmol/L (a–f) Cyanidin-3-*O*-arabinoside (**a**), Cyanidin-3-*O*-galactoside (**b**), Cyanidin-3-*O*-glucoside (**c**) and Cyanidin-3-*O*-Xyloside (**d**)

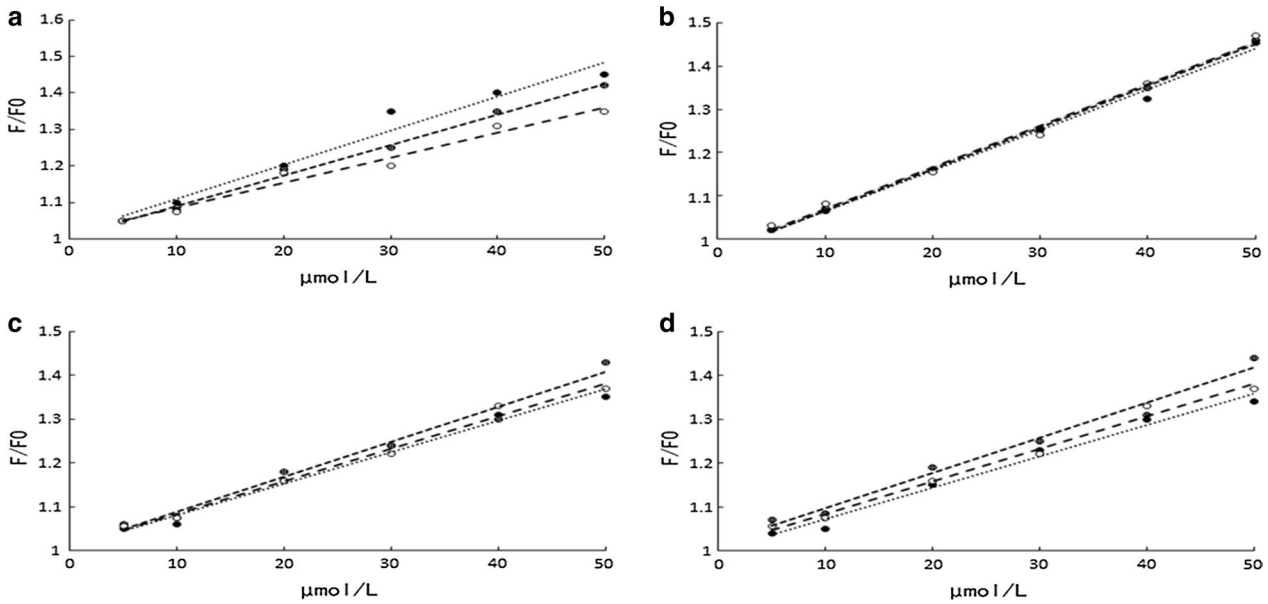

Fig. 2 The Stern–Volmer curves of Cyanidin-3-*O*-arabinoside (**a**), Cyanidin-3-*O*-galactoside (**b**), Cyanidin-3-*O*-glucoside (**c**) and Cyanidin-3-*O*-Xyloside (**d**) at 297, 317 and 337 K

Table 1 The dynamic quenching constants of Cyanidin-3-*O*-arabinoside, Cyanidin-3-*O*-galactoside, Cyanidin-3-*O*-glucoside and Cyanidin-3-*O*-Xyloside at 297, 317 and 337 K

Complexes	T/K	$K_{SV}/(\times 10^3\ L\ mol^{-1})$	$K_q/(\times 10^{11}\ L\ mol^{-1})$
Cyanidin	297	10.227 ± 0.003	10.227 ± 0.003
-3-*O*-	317	9.984 ± 0.156	9.984 ± 0.156
Arabinoside	337	9.166 ± 0.197	9.166 ± 0.197
Cyanidin	297	8.795 ± 0.284	8.795 ± 0.284
-3-*O*-	317	8.699 ± 0.105	8.699 ± 0.105
Galactoside	337	8.012 ± 0.015	8.012 ± 0.015
Cyanidin	297	7.843 ± 0.019	7.843 ± 0.019
-3-*O*-	317	7.435 ± 0.201	7.435 ± 0.201
Glucoside	337	6.915 ± 0.174	6.915 ± 0.174
Cyanidin	297	7.065 ± 0.162	7.065 ± 0.162
-3-*O*-	317	6.845 ± 0.153	6.845 ± 0.153
Xyloside	337	6.254 ± 0.074	6.254 ± 0.074

to C_q. The S-V curve of the protein was in a non-linear relationship, indicating that the quenching of the BSA endogenous fluorescence was not caused by dynamic quenching, possibly due to the formation of non-luminescent complexes between the fluorescent molecules and the quenchers things (Soares et al. 2007).

Dynamic quenching constants of BSA at different temperatures

The dynamic quenching constant K_{SV} of the protein at different temperatures (297, 317 and 337 K) and the dynamic quenching process rate constant Kq were shown in the Table 1. The results showed that when the fluorescence quenching mechanism of the protein was dynamic quenching, K_{SV} generally increased with the temperature of the system, and the maximum diffusion collision quenching constant of the quencher to the biological macromolecule was about 2×10^{10} L Mol^{-1} s^{-1}. It could be seen that the value of K_{SV} decreased with the increase of temperature, and the fluorescence quenching rate constants of the four anthocyanins were much larger than 2×10^{10} L mol^{-1} s^{-1}. It was shown that the quenching mechanism of the four monomer was not a dynamic quenching caused by diffusion and collision, but because of the static quenching caused by the formation of non-luminescent ground state complexes between the fluorescent molecules and the quencher (Sun et al. 2017).

Determination of Binding constants, the number of binding sites and the type of binding

Double logarithmic regression curves of the interaction of four anthocyanins with BSA was shown in Fig. 3 When small molecules bind independently to a set of equivalent sites on a macromolecule, the equilibrium between free and bound molecules is given by the equation Eq. (2).

$$\log(F_0 - F)/F = \log K_s + n \log C_q \quad (2)$$

where K_S and n are the apparent binding constant and the number of binding sites. Thus, a plot (Fig. 3) of log $(F_0 - F)/F$ versus log(Q) yielded the K_S and n values to be 0.574×10^3 L mol^{-1}, 0.484×10^3 L mol^{-1},

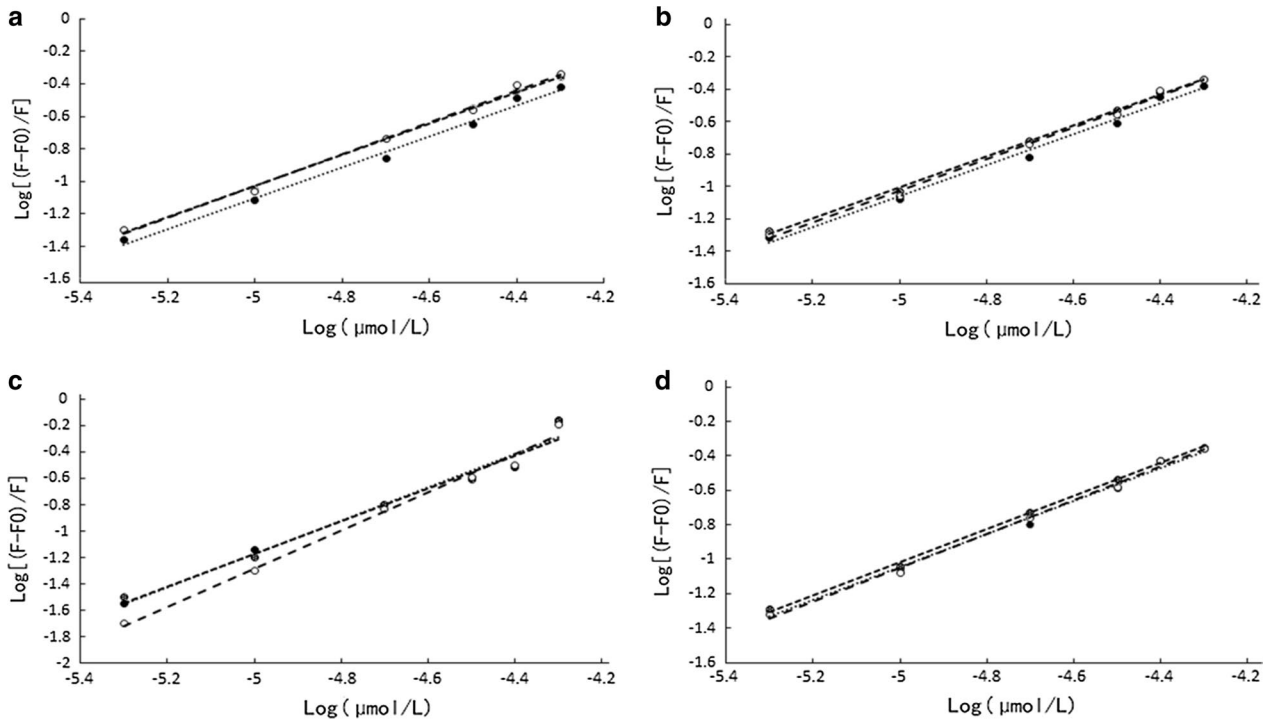

Fig. 3 The double logarithm regression curve of log [($F_0 - F$)/F] versus log [c_q] of Cyanidin-3-*O*-arabinoside (**a**), Cyanidin-3-*O*-galactoside (**b**), Cyanidin-3-i-glucoside (**c**) and Cyanidin-3-*O*-Xyloside (**d**) at 297, 317 and 337 K

Table 2 The binding constants and thermodynamic parameters of Cyanidin-3-*O*-arabinoside, Cyanidin-3-*O*-galactoside, Cyanidin-3-*O*-glucoside and Cyanidin-3-*O*-Xyloside at 297, 317 and 337 K

Complexes	T	K_s (× 10^3 L mol^{-1})	n	ΔH (KJ mol^{-1})	ΔG (KJ mol^{-1})	ΔS (J mol^{-1}· K)
Cyanidin	297	0.574 ± 0.023	0.9395 ± 0.0034	4.03	− 22.39	88.95623
-3-*O*-	317	0.412 ± 0.037	0.9754 ± 0.0044	4.03	− 24.59	90.28391
Arabinoside	337	0.398 ± 0.010	0.9489 ± 0.0058	4.03	− 25.98	89.05045
Cyanidin	297	0.484 ± 0.025	0.9195 ± 0.0054	20.47	− 21.63	86.39731
-3-*O*-	317	0.395 ± 0.011	0.9515 ± 0.0037	20.47	− 20.84	78.45426
Galactoside	337	0.308 ± 0.012	0.9354 ± 0.0014	20.47	− 25.14	86.55786
Cyanidin	297	0.425 ± 0.037	0.9153 ± 0.0022	11.56	− 24.22	95.11785
-3-*O*-	317	0.403 ± 0.033	0.9175 ± 0.0009	11.56	− 29.23	104.9211
Glucoside	337	0.399 ± 0.030	0.9612 ± 0.0074	11.56	− 21.78	76.58754
Cyanidin	297	0.521 ± 0.027	0.9265 ± 0.0085	9.81	− 28.47	109.4276
-3-*O*-	317	0.543 ± 0.026	0.8987 ± 0.0045	9.81	− 23.96	88.29653
Xyloside	337	0.537 ± 0.014	0.9024 ± 0.0049	9.81	− 25.51	87.65579

0.425×10^3 L mol^{-1}, 0.521×10^3 L mol^{-1} and 0.9395, 0.9195, 0.9153, 0.9265 at 297 K as shown in Table 2, respectively. An n value of approximately equal to 1 indicated that there was only a single binding site in the binding of AMA and BSA.

The thermodynamic constants of ligand-macromolecule binding can be calculated according to the Van't Hoff equation Eq. (3)

$$\Delta H = d\left(\frac{\Delta G}{T}\right)/d\left(\frac{1}{T}\right) \quad (3)$$

$$\Delta G = -RT \ln K_s$$

$$\Delta G = \Delta H - T\Delta S$$

wherein the K_S binding constants representative of the temperature T, ΔH, ΔS, ΔG, respectively enthalpy change of the bonding process, entropy and free energy, R is the gas constant (8.314 J mol^{-1} K^{-1}). The values of ΔH, ΔG, and ΔS are listed in Table 2. From the point of view of water structure, a positive ΔS value was frequently taken as evidence for hydrophobic interaction. The negative value of ΔG revealed that the interaction process was spontaneous (Pomar et al. 2005). From the results we can conclude that the ΔG of the binding of the four monomers to BSA was less than 0, indicating that the reaction between the four monomers was spontaneous; ΔH(BSA) > 0, ΔS(BSA) > 0, indicating that the effect of BSA was mainly hydrophobic. ΔH(BSA) > 0, the reaction was endothermic reaction, the K_S value increased with increasing temperature. The interaction forces between a small molecule and macromolecule include hydrogen bonds, van der Waals force, hydrophobic force, electrostatic interactions, etc. In order to elucidate the interaction of AMA with BSA, the thermodynamic parameters were calculated.

Fourier transform infrared spectroscopy (FTIR) analysis

The infrared spectrum was shown in Fig. 4, Changes in the infrared spectrum indicated that the four monomer caused a change in the secondary structure of the BSA. Several oxygen atoms, hydroxyl and BSA C=O, C–N groups through the hydrogen bond, hydrophobic interaction combined to form a complex, resulting in BSA peptide chain rearrangement, and ultimately leaded to secondary structure changes(Hu et al. 2004).

Circular dichroism analysis

Circular dichroic analysis is a useful method for secondary structure estimation of protein molecule. The shape and particular wavelengths of CD spectrums are very sensitive to the secondary structure of proteins. The secondary structure changes of BSA in the presence of the four monomer were studied using circular dichroism spectroscopy. Figure 5 shows CD analysis of BSA in the absence and presence of four monomer, the interaction between AMA and BSA could be verified (Wawer et al. 2006; Slimestad et al. 2005). The four monomer were listed in Table 3 by software, we can conclude that after addition of four monomer, α-helix content of BSA was almost no change, β-fold content was increased, but corner and random curl content was decreased (Karnaukhova 2007). So the CD results demonstrated that the interaction of the four monomer with the BSA leaded to a change in the secondary structure of the BSA, which was consistent with the infrared spectrum (Sahu et al. 2008).

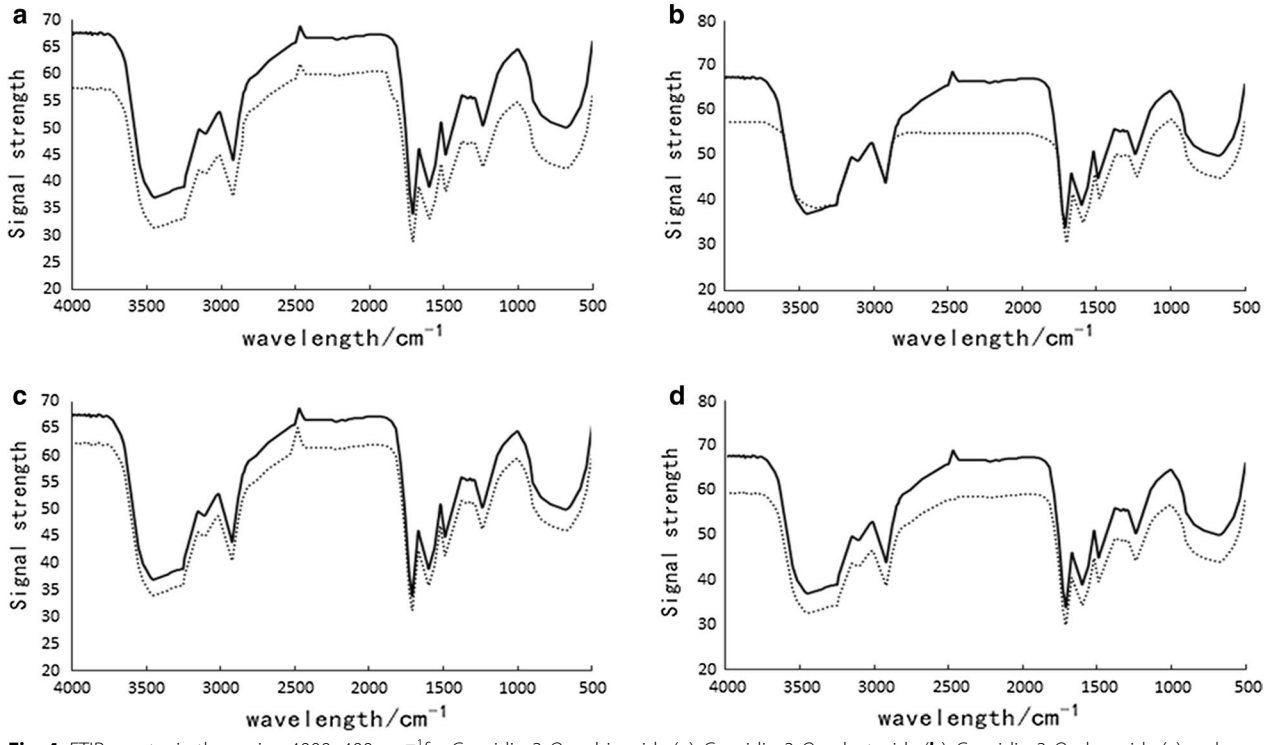

Fig. 4 FTIR spectra in the region 4000–400 $cm^{-1}$for Cyanidin-3-*O*-arabinoside (**a**), Cyanidin-3-*O*-galactoside (**b**), Cyanidin-3-*O*-glucoside (**c**) and Cyanidin-3-*O*-Xyloside (**d**) and their polyphenol complexes

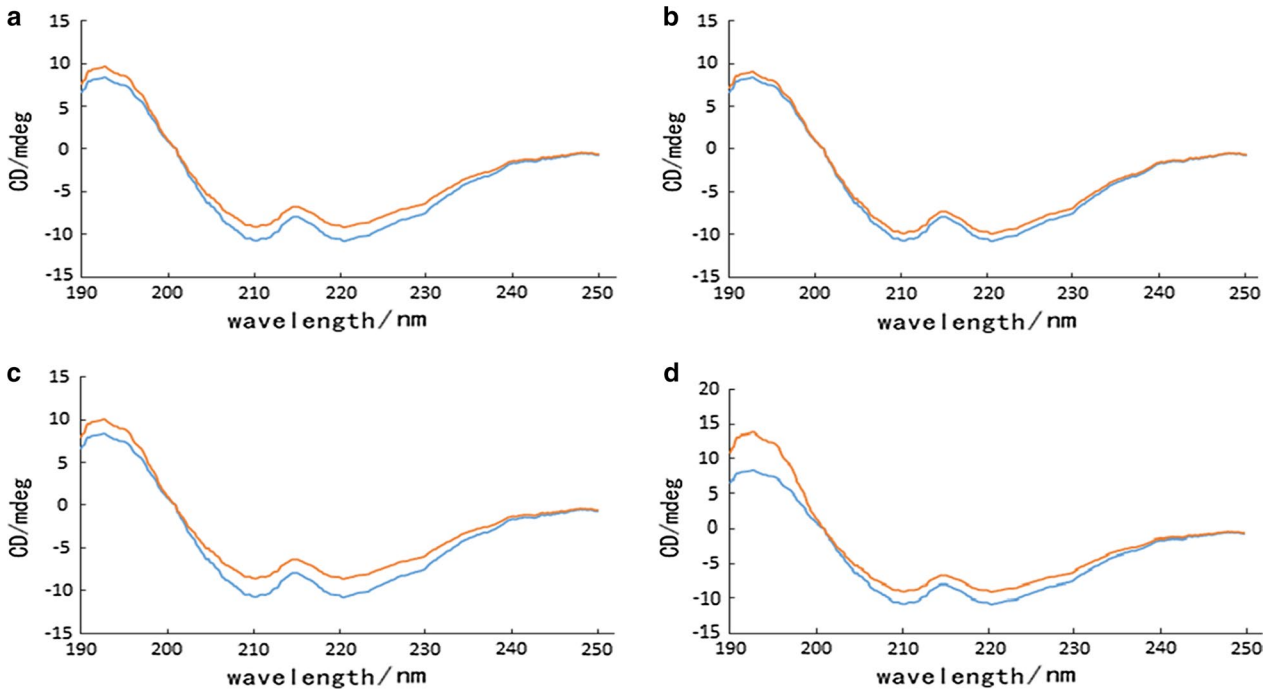

Fig. 5 The far-UV CD spectra of Cyanidin-3-*O*-arabinoside (**a**), Cyanidin-3-*O*-galactoside (**b**), Cyanidin-3-*O*-glucoside (**c**) and Cyanidin-3-*O*-Xyloside (**d**) in absence and presence of BSA

Table 3 Secondary structure analysis from the BSA and AMA

AMA (10 μmol L^{-1})	α-helix (%)	β-fold (%)	β-angle (%)	Random curl (%)
BSA	10.2	9.1	33.2	47.5
With cyanidin-3-*O*-arabinoside	9.2	8.9	35.0	46.9
With cyanidin-3-*O*-galactoside	9.0	9.1	34.7	47.2
With cyanidin-3-*O*-glucoside	9.1	8.8	34.1	48.0
with cyanidin-3-*O*-Xyloside	9.2	8.9	33.9	48.0

Computational analysis of the binding between AMA and BSA

We carried out docking simulations to investigate the possible 4 anthocyanins-binding site on BSA. The binding energy of 50 models in docking is shown in Fig. 6. In areas where these binding patterns are present, AMA may bind to BSA and is located in the region shown in Fig. 6. Consequently, the stabilizing effect contributed by AMA on the appendant structure of BSA may prevent the occurrence of domain swapping, so as to redirect BSA away from the fibril-forming pathway and into forming nontoxic, unstructured, and off-pathway aggregates (Gao et al. 2005). So we speculated that AMA could inhibit the fibrillation of BSA complex in this study. The observation was particular significance as these four anthocyanins had higher stability after interacting with BSA.

Discussion

It is reported that the content of AMA is up to 1%, far higher than other plants (Olszewska and Michel 2009), so in this paper, the aim of above research is to clarify the binding mechanism of AMA with BSA, we will provide valuable information about interaction of AMA as a plant-based food additives with BSA as an important carrier protein, this is of great significance for the follow-up study of AMA and BSA (Li et al. 2016), and we also provide useful information for understanding the Pharmacological effects at molecular level (Zhang et al. 2012).

A series of multispectral technology and molecular docking studies, including interaction was used to analyze AMA and BSA. Fluorescence quenching showed that AMA can quench the fluorescence intensity of BSA through static mechanism making it possible to study the

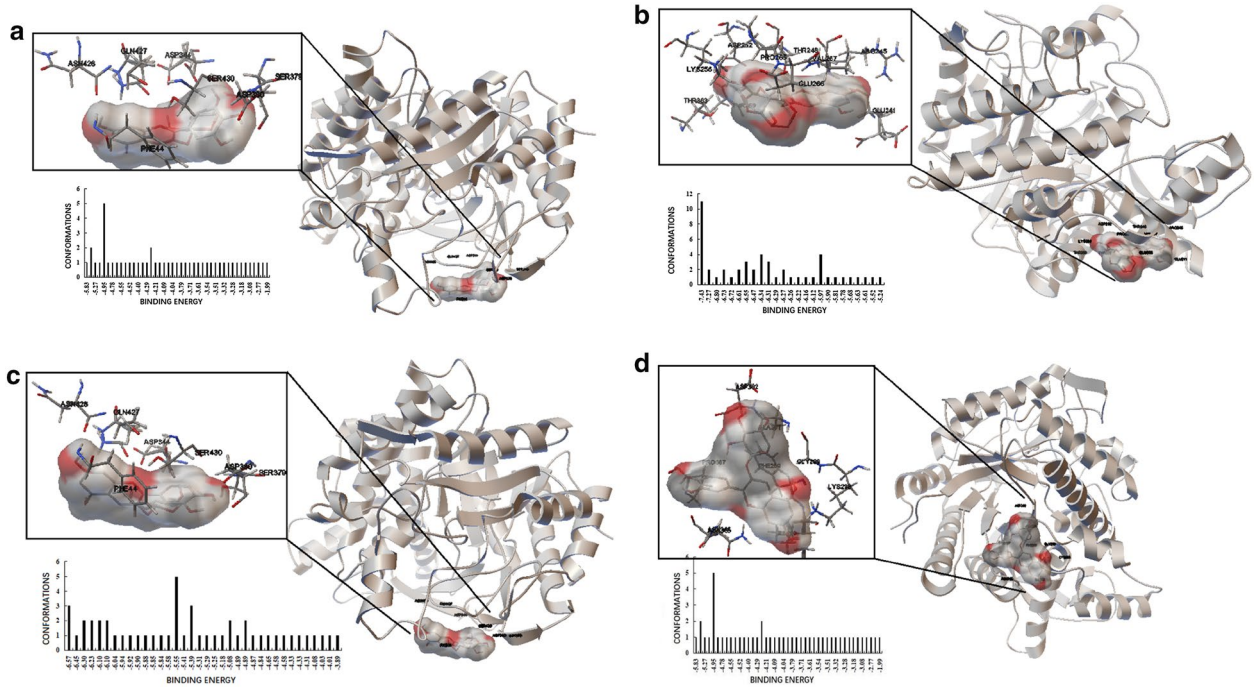

Fig. 6 Use Autodock software binding energy of 50 docking models. Panoramic view showing the binding mode between Cyanidin-3-*O*-arabinoside (**a**), Cyanidin-3-*O*-galactoside (**b**), Cyanidin-3-*O*-glucoside (**c**) and Cyanidin-3-*O*-Xyloside (**d**), and BSA

interaction of AMA with this protein using Stern–Volmer equation.

The results obtained from FTIR to CD showed that the α-helix content of BSA did not change significantly in the absence and presence of the four monomer, and the content of β-sheet was increased and the curvature and random curl content were decreased. The interaction of the four substance with BSA resulted the changes of BSA in the conformation and secondary structure. According to the Förster's non-radiative energy transfer theory, the binding distance r between AMA and BSA was calculated, the result represents a static quenching, and the binding reaction is spontaneous and is largely mediated by hydrophobic forces.

Molecular docking is a key tool in structural molecular biology. The goal of ligand–protein docking is to predict the predominant binding mode(s) of a ligand with a protein of known three-dimensional structure (Morris and Lim-Wilby 2008). The obtained molecular docking results indicated that AMA can interact with BSA, without breaking the secondary structure of BSA. Conformational studies of BSA indicate that Trp212 is involved in the interfacial formation of subdomains IIA and IIIA and that the two hydrophobic cavities are the major regions where small molecule compounds bind to proteins through molecular modeling, several anthocyanins share the same binding site. In view of above this, it is of great significance to study the combination of AMA/BSA through the multi-spectral and molecular docking described.

Abbreviations

MD: molecular dynamic simulations; AMA: anthocyanins in *Aronia melanocarpa*; BSA: bovine serum albumin; CD: circular dichroism spectroscopy; FTIR: Fourier transform infrared spectroscopy.

Authors' contributions

WJ and WQY conceived and designed the study. XDX performed the experiments and wrote the manuscript. YJ and ZX reviewed and edited the manuscript. All authors read and approved the manuscript.

Acknowledgements

This research was supported by the National Natural Science Foundation of China (Grant No. 31701656).

Competing interests

The authors declare that they have no competing interests.

Availability of data and materials

Not applicable.

Consent for publication

Not applicable.

Ethics approval and consent to participate

Not applicable.

Funding

Not applicable.

Publisher's Note

Received: 21 April 2018 Accepted: 25 April 2018
Published online: 02 May 2018

References

Chrubasik C, Li G, Chrubasik S (2010) The clinical effectiveness of chokeberry: a systematic review. Phytother Res 24(8):1107. https://doi.org/10.1002/ptr.3226

de Santiago MCPA, Gouvêa ACMS, de Oliveira RLO, Borguini RG, Pacheco S, Nogueira RI, da de do Nascimento LSM, Freitas SP (2014) Analytical standards production for the analysis of pomegranate anthocyanins by HPLC. Braz J Food Technol 17(1):51–57. https://doi.org/10.1590/bjft.2014.008

Fares R, Bazzi S, Baydoun SE, Abdel-Massih RM (2011) The antioxidant and anti-proliferative activity of the Lebanese *Olea europaea* extract. Plant Foods Hum Nutr 66(1):58–63. https://doi.org/10.1007/s11130-011-0213-9

Gallo M, Vinci G, Graziani G, De Simone C, Ferranti P (2013) The interaction of cocoa polyphenols with milk proteins studied by proteomic techniques. Food Res Int 54(1):406–415. https://doi.org/10.1016/j.foodres.2013.07.011

Gao D, Tian Y, Bi S, Chen Y, Aimin Yu, Zhang H (2005) Studies on the interaction of colloidal gold and serum albumins by spectral methods. Spectrochim Acta A 62(4–5):1203–1208. https://doi.org/10.1016/j.saa.2005.04.026

Hassellund SS, Flaa A, Sandvik L, Kjeldsen SE, Rostrup M (2012) Effects of anthocyanins on blood pressure and stress reactivity: a double-blind randomized placebo-controlled crossover study. J Hum Hypertens 26(6):396–404. https://doi.org/10.1038/jhh.2011.41

Hu YJ, Liu Y, Wang JB, Xiao XH, Qu SS (2004) Study of the interaction between monoammonium glycyrrhizinate and bovine serum albumin. J Pharmaceut Biomed 36(4):915–919. https://doi.org/10.1016/j.jpba.2004.08.021

Karnaukhova E (2007) Interactions of human serum albumin with retinoic acid, retinal and retinyl acetate. Biochem Pharmacol 73(6):901–910. https://doi.org/10.1016/j.bcp.2006.11.023

Kokotkiewicz A, Jeremicz Z, Luczkiewicz M (2010) *Aronia* plants: a review of traditional use, biological activities, and perspectives for modern medicine. J Med Food 13(3):255–269. https://doi.org/10.1089/jmf.2009.0062

Li T, Cheng Z, Cao L, Jiang X, Fan L (2016) Data of fluorescence, UV–vis absorption and FTIR spectra for the study of interaction between two food colourants and BSA. Data Brief 8(C):755–783. https://doi.org/10.1016/j.dib.2016.06.025

Malinowska J, Oleszek W, Stochmal A, Olas B (2013) The polyphenol-rich extracts from black chokeberry and grape seeds impair changes in the platelet adhesion and aggregation induced by a model of hyperhomocysteinemia. Eur J Nutr 52(3):1049–1057. https://doi.org/10.1007/s00394-012-0411-8

Manikandamathavan VM, Thangaraj M, Weyhermuller T, Parameswari RP, Murthy NN, Punitha, Nair BU (2017) Novel mononuclear Cu (II) terpyridine complexes: impact of fused ring thiophene and thiazole head groups towards DNA/BSA interaction, cleavage and antiproliferative activity on HepG2 and triple negative CAL-51 cell line. Eur J Med Chem 135:434–446. https://doi.org/10.1016/j.ejmech.2017.04.030

Morris GM, Lim-Wilby M (2008) Molecular docking. Methods Mol Biol 443(443):365–382

Olszewska MA, Michel P (2009) Antioxidant activity of inflorescences, leaves and fruits of three *Sorbus* species in relation to their polyphenolic composition. Nat Prod Res 23(16):1507–1521

Paul S, Sepay N, Sarkar S, Roy P, Dasgupta S, Sardar PS, Majhi A (2017) Interaction of serum albumins with fluorescent ligand 4-azido coumarin: spectroscopic analysis and molecular docking studies. New J Chem 41(24):15392–15404. https://doi.org/10.1039/C7NJ02335A

Pomar F, Novo M, Masa A (2005) Varietal differences among the anthocyanin profiles of 50 red table grape cultivars studied by high performance liquid chromatography. J Chromatogr A 1094(1–2):34. https://doi.org/10.1016/j.chroma.2005.07.096

Sahu A, Kasoju N, Bora U (2008) Fluorescence study of the curcumin-casein micelle complexation and its application as a drug nanocarrier to cancer cells. Biomacromolecules 9(10):2905–2912. https://doi.org/10.1021/bm800683f

Sedighipoor M, Kianfar AH, Mahmood WAK, Azarian MH (2017) Synthesis and electronic structure of novel schiff bases Ni/Cu (II) complexes: evaluation of DNA/Serum protein binding by spectroscopic studies. Polyhedron 129:1–8. https://doi.org/10.1016/j.poly.2017.03.027

Slimestad R, Torskangerpoll K, Nateland HS, Johannessen T, Giske NH (2005) Flavonoids from black chokeberries. *Aronia melanocarpa*. J Food Compos Anal 18(1):61–68. https://doi.org/10.1016/j.jfca.2003.12.003

Soares S, Mateus N, De Freitas V (2007) Interaction of different polyphenols with bovine serum albumin (BSA) and human salivary alpha-amylase (HSA) by fluorescence quenching. J Agric Food Chem 55(16):6726–6735. https://doi.org/10.1021/jf070905x

Sun L, Gidley MJ, Warren FJ (2017) The mechanism of interactions between tea polyphenols and porcine pancreatic alpha-amylase: analysis by inhibition kinetics, fluorescence quenching, differential scanning calorimetry and isothermal titration calorimetry. Mol Nutr Food Res 61(10):1613. https://doi.org/10.1002/mnfr.20170032

Unnikrishnan B, Wei SC, Chiu WJ, Cang J, Hsu PH, Huang CC (2014) Nitrite ion-induced fluorescence quenching of luminescent BSA-Au(25) nanoclusters: mechanism and application. Analyst 139(9):2221–2228. https://doi.org/10.1039/c3an02291a

Wawer I, Wolniak M, Wawer Paradowska K I (2006) Solid state NMR study of dietary fiber powders from *Aronia*, bilberry, black currant and apple. Solid State Nucl Magn Reson 30(2):106–113. https://doi.org/10.1016/j.ssnmr.2006.05.001

Wei J, Zhang G, Zhang X, Gao J, Fan J, Zhou Z (2016) Anthocyanin improving metabolic disorders in obese mice from *Aronia melanocarpa*. Indian J Pharm Educ Res 50(3):368–375. https://doi.org/10.5530/ijper.50.3.8

Wei J, Zhang G, Zhang X, Xu D, Gao J, Fan J, Zhou Z (2017) Anthocyanins from black chokeberry (*Aronia melanocarpa* Elliot) delayed aging-related degenerative changes of brain. J Agric Food Chem 65(29):5973–5984. https://doi.org/10.1021/acs.jafc.7b02136

Zhang G, Wang A, Jiang T, Guo J (2008a) Interaction of the irisflorentin with bovine serum albumin: a fluorescence quenching study. J Mol Struct 891(1–3):93–97. https://doi.org/10.1016/j.molstruc.2008.03.002

Zhang Y-Z, Zhou B, Liu Y-X, Zhou C-X, Ding X-L, Liu Y (2008b) Fluorescence study on the interaction of bovine serum albumin with *P*-aminoazobenzene. J FLUORESC 18(1):109–118. https://doi.org/10.1007/s10895-007-0247-4

Zhang G, Ma Y, Wang L, Zhang Y, Zhou J (2012) Multispectroscopic studies on the interaction of maltol, a food additive, with bovine serum albumin. Food Chem 133(2):264–270. https://doi.org/10.1016/j.foodchem.2012.01.014

Zhang J, Zhuang S, Tong C, Liu W (2013) Probing the molecular interaction of triazole fungicides with human serum albumin by multispectroscopic techniques and molecular modeling. J Agric Food Chem 61(30):7203–7211. https://doi.org/10.1021/jf401095n

Zhang X, Li M, Wang Y, Zhao Y (2015) Insight into the binding mode of a novel LSD1 inhibitor by molecular docking and molecular dynamics simulations. J Recept Signal Transduct 35(5):363–369. https://doi.org/10.3109/10799893.2015.1049360